

## Single-Molecule Surface-Enhanced Raman Spectroscopy of Nonresonant Molecules

Evan J. Blackie, Eric C. Le Ru, and Pablo G. Etchegoin\*

*The MacDiarmid Institute for Advanced Materials and Nanotechnology, School of Chemical and Physical Sciences, Victoria University of Wellington, P.O. Box 600, Wellington, New Zealand*

Received July 2, 2009; E-mail: pablo.etchegoin@vuw.ac.nz

**Abstract:** Single-molecule surface-enhanced Raman scattering (SERS) detection of nonresonant molecules is demonstrated experimentally using the bianalyte SERS method. To this end, bianalyte SERS is performed at 633 nm excitation using the nonresonant molecule 1,2-di-(4-pyridyl)-ethylene (BPE) in combination with a benzotriazole derivative as a partner. The results are then extended to the even more challenging case of a small nonresonant molecule, adenine, using an isotopically substituted adenine as bianalyte SERS partners. In addition, SERS cross sections of single-molecule events are quantified, thus providing estimates of the enhancement factors needed to see them. It turns out that an enhancement factor on the order of  $\sim 5 \times 10^9$  was sufficient for single-molecule detection of BPE, while maximum enhancement factors of  $\sim 5 \times 10^{10}$  were observed in extreme cases. In the case of adenine, single-molecule detection was only possible in the rare cases with enhancement factors of  $\sim 10^{11}$ . This study constitutes a quantitative fundamental test into the lowest detection limits (in terms of differential cross sections) for single-molecule SERS.

### Introduction

The bianalyte approach<sup>1</sup> offers one of the most versatile methods for identifying single-molecule events in surface-enhanced Raman scattering (SERS),<sup>2,3</sup> as shown in many recent studies.<sup>4–10</sup> In addition to single-molecule studies, such experiments will eventually provide further insights into the finer details of the enhancement factor (EF) distribution at hot spots, a topic which has been the subject of intense study in both SERS<sup>11–14</sup> and tip-enhanced Raman scattering (TERS).<sup>15</sup>

The bianalyte technique<sup>1</sup> has largely been used so far with *resonant* or *preresonant* molecules at a given laser excitation (typically in the red or green regions of the spectrum). This includes experiments with isotopically substituted rhodamine derivatives in refs 8–10. Hence, starting differential cross sections of the bare probes are on the order of  $\sim 10^{-27}$  cm<sup>2</sup>/sr for the most intense Raman modes. This presents a huge advantage with respect to the minimum enhancement factor that is required to observe single-molecule events under typical experimental conditions of laser power densities and integration times (which have to be compatible with the photostability of the probes<sup>10</sup>). SERS enhancement factors on the order of  $\sim 10^8$  are more than enough to observe SM-SERS in this situation.<sup>7,10,16,17</sup> A comprehensive discussion on the topic of the minimum enhancement factor needed for single-molecule detection has been recently given in ref 16 and will be used as reference material for part of the discussion.

Electromagnetic SERS EFs at hot spots are predicted to be on the order of  $\sim 10^{10}–10^{11}$ , for example at a junction between metallic particles<sup>3,11,16,18–21</sup> or at the tip of small elongated particles.<sup>3,22</sup> Enhancement factors of this order may not in some cases be measured in single-molecule events of resonant or preresonant molecules because of photobleaching.<sup>10</sup> However, it should be possible to use these expected large enhancements ( $\sim 10^{10}–10^{11}$ ) to bridge the gap between resonant or preresonant

- (1) Ru, E. C. L.; Meyer, M.; Etchegoin, P. G. *J. Phys. Chem. B* **2006**, *110*, 1944.
- (2) Aroca, R. F. *Surface-Enhanced Vibrational Spectroscopy*; John Wiley & Sons: Chichester, 2006.
- (3) Le Ru, E. C.; Etchegoin, P. G. *Principles of Surface Enhanced Raman Spectroscopy and Related Plasmonic Effects*; Elsevier: Amsterdam, 2009.
- (4) Sawai, Y.; Takimoto, B.; Nabika, H.; Ajito, K.; Murakoshi, K. *J. Am. Chem. Soc.* **2007**, *129*, 1658.
- (5) Goulet, P. J. G.; Aroca, R. F. *Anal. Chem.* **2007**, *79*, 2728.
- (6) Etchegoin, P. G.; Meyer, M.; Blackie, E.; Le Ru, E. C. *Anal. Chem.* **2007**, *79*, 8411.
- (7) Le Ru, E. C.; Blackie, E.; Meyer, M.; Etchegoin, P. G. *J. Chem. Phys. C* **2007**, *111*, 13794.
- (8) Dieringer, J. A.; II, R. B. L.; Scheidt, K. A.; Duynes, R. P. V. *J. Am. Chem. Soc.* **2007**, *129*, 16249.
- (9) Blackie, E.; Le Ru, E. C.; Meyer, M.; Timmer, M.; Burkett, B.; Northcote, P.; Etchegoin, P. G. *Phys. Chem. Chem. Phys.* **2008**, *10*, 4147.
- (10) Etchegoin, P. G.; Lacharmoise, P. D.; Le Ru, E. C. *Anal. Chem.* **2009**, *81*, 682.
- (11) Le Ru, E. C.; Etchegoin, P. G.; Meyer, M. *J. Chem. Phys.* **2006**, *125*, 204701.
- (12) Etchegoin, P. G.; Meyer, M.; Le Ru, E. C. *Phys. Chem. Chem. Phys.* **2007**, *9*, 3006.
- (13) Fang, Y.; Seong, N.-H.; Dlott, D. D. *Science* **2008**, *321*, 388.
- (14) Le Ru, E. C.; Etchegoin, P. G. *J. Chem. Phys.* **2009**, *130*, 181101.
- (15) Domke, K. F.; Zhang, D.; Pettinger, B. *J. Phys. Chem. C* **2007**, *111*, 8611.

- (16) Etchegoin, P. G.; Le Ru, E. C. *Phys. Chem. Chem. Phys.* **2008**, *10*, 6079.
- (17) Pieczonka, N. P. W.; Aroca, R. F. *Chem. Soc. Rev.* **2008**, *37*, 946.
- (18) Xu, H.; Aizpurua, J.; Käll, M.; Apell, P. *Phys. Rev. E* **2000**, *62*, 4318.
- (19) Li, K. R.; Stockman, M. I.; Bergman, D. J. *Phys. Rev. Lett.* **2003**, *91*, 227402.
- (20) Johansson, P.; Xu, H.; Käll, M. *Phys. Rev. B* **2005**, *72*, 035427.
- (21) Etchegoin, P. G.; Galloway, C.; Le Ru, E. C. *Phys. Chem. Chem. Phys.* **2006**, *8*, 2624.
- (22) Boyack, R.; Le Ru, E. C. *Phys. Chem. Chem. Phys.* **2009**, *11*, 7398.

dyes and nonresonant molecules, which can have differential cross sections in the typical range of  $\sim 10^{-29}$ – $10^{-30}$  cm<sup>2</sup>/sr. Raman differential cross sections on the order of  $\sim 10^{-30}$  cm<sup>2</sup>/sr in the visible are among the smallest values we can find in molecules (except perhaps for diatomic gases like N<sub>2</sub>, which has a cross section of  $\sim 2 \times 10^{-31}$  cm<sup>2</sup>/sr at 633 nm excitation). In this context, the bianalyte SERS technique can help to pin down single-molecule cases in situations that can be described informally as a “worst case scenario” as far as the bare differential cross sections of the probes is concerned. It is therefore a fundamental test into the lowest detection limits of the technique at the single-molecule level and offers, in principle, an answer to the crucial question: “*can any molecule be detected at the single-molecule level with SERS?*”. In fact, nonresonant molecules represent a large group of interest including biological molecules and many common chemicals of interest for environmental and/or forensic science. In terms of potential applications of SERS to chemical detection, accordingly, the lower detection limit is of great interest and constitutes an important claim for the universality and applicability of the technique as a whole.

In this paper, we shall present a demonstration of bianalyte SERS with nonresonant probes. It is worth highlighting that claims of single-molecule detection of nonresonant probes have been made in the past; for example, refs 23 and 24 have claimed single-adenine detection with SERS based on either “blinking” or “ultralow concentration” approaches. The difference in the reliability between these latter techniques and a “contrast” method like bianalyte SERS has been extensively discussed in refs 1, 7, 11, and 12 and will not be repeated here. Moreover, ref 23 makes no attempt to quantify the observed cross sections but rather points out that blinking might be considered as evidence for single-molecule sensitivity, while ref 24 works at ultralow concentrations ( $\sim 30$  pM) and derives estimates of cross sections from vibrational pumping at room temperature, which are notoriously inaccurate due mainly (but not exclusively) to laser heating effects and nonradiative contributions to the cross section (both discussed recently in ref 25). The problems associated with the estimation of cross sections in this way have been further evidenced in recent studies of SERS vibrational pumping at the single-molecule level.<sup>26</sup>

Accordingly, we believe that the field is still lacking a convincing demonstration of single-molecule SERS for nonresonant molecules and, by the same token, a quantitative assessment of the lowest possible single-molecule detection limit that is achievable in practice. Hence, the study in this paper is focused toward filling what we perceive as an existing gap in the “proofs of principle” of the technique. We shall show that single-molecule detection of probes with bare differential cross sections on the order of  $d\sigma/d\Omega \approx 10^{-30}$  cm<sup>2</sup>/sr is indeed possible but substantially more complicated than a simple “rescaling” of the problem for molecules with much larger  $d\sigma/d\Omega$ 's, for several new “interfering effects” arise and make the experimental determination considerably more challenging. As such, a careful optimization of the SERS substrate and conditions is necessary to remediate (or partially compensate) such effects.

We shall commence by describing the problem in several stages to understand the origin of the additional complications of nonresonant bianalyte SERS.

**General Considerations.** If we were able to integrate the signal of a single molecule for an unlimited amount of time ( $\tau$ ) and for an arbitrarily large laser power density ( $I_L$ ), we would then be able to eventually reveal the signal above a minimum signal-to-noise ratio (SNR) and measure the spectrum of a single molecule without any enhancement. Obviously this is not possible, and there are intrinsic limitations to how much power density and integration time we can use. In fact, a more important parameter—as far as the photostability of the probe is concerned, i.e. photobleaching—is the product of the laser power density and the integration time ( $I_L \times \tau$ ). But limitations in integration time can arise by themselves without necessarily being linked to photobleaching. Liquid samples, for example, are limited by the diffusion time of the colloids in the scattering volume of the objective. Other instabilities of the signal (often categorized under the broad umbrella of “blinking”) can exist. The latter comprise a whole variety of processes that go from molecular surface diffusion to subtle changes in the geometry of the SERS substrate. Accordingly, having limitations in the maximum  $I_L$ 's and  $\tau$ 's we can use, there is an intrinsic limitation to how much signal we can obtain from a single molecule; the gap bridging this value with the minimum signal we can distinguish above the noise level must then be provided by the SERS enhancement.<sup>16</sup> For our purposes here, when we talk about “characteristic values” of the enhancement needed to see single molecules, we are implicitly assuming also “characteristic experimental conditions” for real molecules as far as both  $I_L$  and  $\tau$  are concerned. The values should then be understood in that context. A more in-depth discussion of typical experimental limitations for minimum cross sections has been given in ref 16.

**Statistics and Enhancement Factor Distribution.** The spatial distribution of the enhancement factor around hot spots (where single-molecule signals typically originate) has been studied in full detail before.<sup>11,12,14</sup> The probability of having a certain SERS enhancement factor  $F$  in a typical SERS substrate with hot spots follows a long-tail distribution, as schematically depicted in Figure 1. This type of long-tail probability distribution, which has its origin in the extreme variations of the spatial distribution of the enhancements at hot spots, is responsible for a big fraction of the phenomenology of single-molecule SERS statistics observed in experiments. Molecules with differential cross sections in the range  $\sim 10^{-27}$  cm<sup>2</sup>/sr can be readily observed as single molecules for enhancements around and above  $\sim 10^8$  (in the sense explained at the beginning of this section; i.e. for characteristic values of  $I_L \times \tau$ ). Photobleaching may in some cases prevent observation of enhancements larger than  $\sim 10^8$ – $10^9$  (depending again on  $I_L$  and  $\tau$ ).<sup>10</sup> Nonresonant molecules, on the other hand, with differential cross sections on the order of  $\sim 10^{-30}$  cm<sup>2</sup>/sr, require an additional boost of  $\sim 10^3$  to the enhancement factor to be observed as single-molecule events (assuming the same experimental conditions used to see resonant single molecules at  $\sim 10^8$  enhancement). Thus, SM-SERS in this latter case can only arise from regions with the largest enhancements available in the distribution, at  $\sim 10^{11}$ . Note that, in principle, since nonresonant molecules are less subject to photobleaching (although not completely immune from it, see ref 13), this figure may be partly reduced in some cases by adjusting  $I_L$  and  $\tau$ .

(23) Maruyama, Y.; Ishikawa, M.; Futamata, M. *Chem. Lett.* **2001**, *30*, 834.

(24) Kneipp, K.; Kneipp, H.; Kartha, V. B.; Manoharan, R.; Deinum, G.; Itzkan, I.; Dasari, R. R.; Feld, M. S. *Phys. Rev. E* **2001**, *57*, R6281.

(25) Maher, R. C.; Galloway, C. M.; Le Ru, E. C.; Cohen, L. F.; Etchegoin, P. G. *Chem. Soc. Rev.* **2008**, *37*, 965.

(26) Galloway, C.; Le Ru, E. C.; Etchegoin, P. G. *Phys. Chem. Chem. Phys.* **2009**, *11*, 7372.

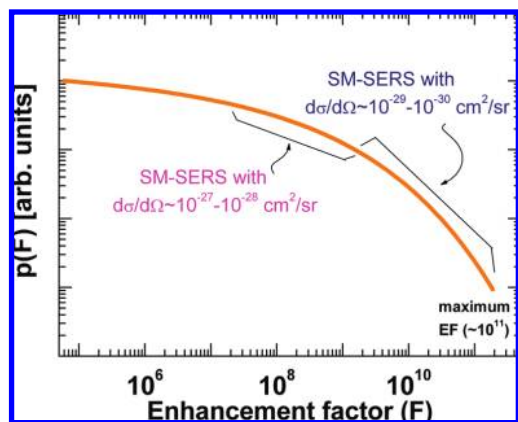


**Figure 1.** Typical long-tail probability distribution for the SERS enhancement factor, for SERS substrates suitable for single-molecule detection.<sup>14</sup> Molecules with differential cross sections  $\sim 10^{-27}$   $\text{cm}^2/\text{sr}$  are observable as single molecules above  $F \approx 10^8$  for typical experimental conditions,<sup>7</sup> while nonresonant molecules with  $d\sigma/d\Omega \approx 10^{-30}$   $\text{cm}^2/\text{sr}$  require typical enhancements of  $\sim 10^{11}$ , at the high end of the distribution (and therefore of rare occurrence).

This basic “change of scale” in the problem (when going from resonant or preresonant molecules to nonresonant ones) introduces new peculiarities. From the purely electromagnetic point of view, there is a much narrower range of enhancements that are “usable” at the very top of the distribution to push signals above the minimum signal-to-noise ratio (SNR), or to put it differently there is a much smaller *effective area* of the hot spots that is usable (around the maximum) that provides enough enhancement to produce an SM-SERS signal.<sup>16</sup> Accordingly, the statistics becomes much sparser. Expressed in a different manner: a much finer “tuning” of the conditions to see single molecules is required when we need to exploit the largest available enhancements close to the cutoff of the distribution.

**Contamination Issues.** We have so far only covered basic electromagnetic aspects of the problem, but there are additional experimental complications produced by the “change in scale” in the required enhancements for single-molecule SERS detection. One of the main problems for single-molecule SERS experiments for probes with  $d\sigma/d\Omega \approx 10^{-30}$   $\text{cm}^2/\text{sr}$  is that *there are many other spurious competing molecules with similar (weak) differential cross sections* normally present in standard experimental conditions. This is particularly true for organic molecules (which include most common SERS probes). This is not obviously a problem for resonant or preresonant dyes, because the single-molecule signals are completely dominated by these, owing to their much higher intrinsic cross sections. Single molecules can be observed in this last case while signals from nonresonant molecules are completely buried in the noise. But the competition with signals from impurities certainly does become an issue for nonresonant molecules. In some cases, these spurious signals arise from molecules that are present in the system via the synthetic route of the SERS substrate. An example of this problem is the presence of *citrate* molecules, which are used in the Lee and Meisel recipe for silver and gold colloids as a reducing/stabilizing agent.<sup>27</sup> These undesirable organic species have cross sections comparable to those of the nonresonant analyte, thus complicating the analysis of the signals. To minimize such contaminants, it was necessary to optimize the SERS substrate preparation and conditions. For

this reason, instead of Lee and Meisel colloids, we have used those synthesized by a simple borohydride reduction, as described later. Even then, the inclusion of organic impurities during substrate/sample preparation/handling is not easy to control, and contamination problems at the single-molecule level are therefore very difficult to avoid.

The problem, in fact, is more acute than the mere presence of undesirable organic species, for these molecules, particularly on dried substrates, are normally susceptible to photodecomposition, thus creating “dynamic species” that change over time. The latter problem has been studied in some detail by several authors<sup>28–30</sup> and leads ultimately (at high powers) to the well-known *amorphous carbon-like* spectral features<sup>31</sup> (a “double dome” at  $\sim 1500$   $\text{cm}^{-1}$  superimposed sometimes with sharper peaks for specific individual spectra<sup>30</sup>).

## Experimental Details

For all the reasons described above, bioanalyte SERS (BiASERS) for nonresonant molecules is considerably more challenging than a mere “scaling” of the problem for resonant or preresonant probes. It means that experimental conditions, including choice of SERS probes and SERS substrate, along with data analysis techniques, must be precisely adjusted to meet the new demands of the problem.

**Raman and SERS Experiments.** For all Raman/SERS experiments, a Jobin-Yvon LabRam Raman microscope in a standard backscattering configuration was used with a 633 nm HeNe laser. For the measurement of bare Raman cross sections, a  $\times 100$  Olympus water immersion objective ( $NA = 1.0$ ) was used. Resolvable peaks from the bare Raman spectra (after subtraction of the measured solvent background) were fitted using pseudo-Voigt functions, and the integrated intensity was compared to that of the reference (the 516  $\text{cm}^{-1}$  peak of 2-bromo-2-methylpropane taken under identical conditions) to give the estimated differential cross section of analytes as explained in ref 7.

Since the SERS measurements are carried out in air, it is necessary to compute the SERS EF by comparison with the bare Raman cross section of the analyte as measured in the gas phase.<sup>3</sup> Such measurements are often difficult, and we therefore estimate the gas-phase Raman cross section by dividing the solvent Raman cross section by the local field correction factor  $L = ((n^2 + 2)/3)^4$  where  $n$  is the refractive index of the solvent.<sup>3,7</sup> This correction is not negligible,  $L = 2.5$  in water and  $L = 2.7$  in ethanol, but must be applied in order to follow a rigorous definition of the SERS EFs<sup>3,7</sup> and to make a like-to-like comparison with electromagnetic calculations.

For the SERS experiments on solid substrates, a  $\times 50$  Olympus long working-distance objective ( $NA = 0.5$ ) was used, and maps were taken of selected areas to give a large statistical sample of events. Raman maps are performed on completely independent spots separated by more than 1  $\mu\text{m}$  using an automated X-Y stage. When a single-molecule event is detected, we cannot identify the exact location of the molecule within the diffraction-limited spot of the laser (which has been measured to be  $\sim 650$  nm in diameter for our system). The deduced cross sections are interpreted in terms of the average power density in the spot, a standard practice in Raman microscopy (also used in ref 7). Single-molecule enhancement factors (SMEF) were obtained after a characterization of the optical setup on the day of the experiments. The scattering volume of the objective used in the SERS experiments was estimated according to the procedure described in the Supporting Information of ref 7, i.e. by measuring the axial and confocal pinhole dependence of the intensity on a Si wafer. The measured effective scattering

(28) Kudelski, A.; Pettinger, B. *Chem. Phys. Lett.* **2000**, *321*, 356.

(29) Bjerneld, E. J.; Svedberg, F.; Johansson, P.; Käll, M. *J. Phys. Chem. A* **2004**, *108*, 4187.

(30) Le Ru, E. C.; Etchegoin, P. G. *Chem. Phys. Lett.* **2004**, *396*, 393.

(31) Otto, A. *J. Raman Spectrosc.* **2002**, *33*, 593.

(27) Lee, P.; Meisel, D. *J. Phys. Chem.* **1982**, *86*, 3391.

**Table 1.** Main Raman Active Modes of BPE (in Ethanol), BTZ (in Water), Adenine (In Water), and  $^{15}\text{N}$ -Adenine (in Water) along with Their Experimentally Determined Non-SERS Cross Sections<sup>a</sup>

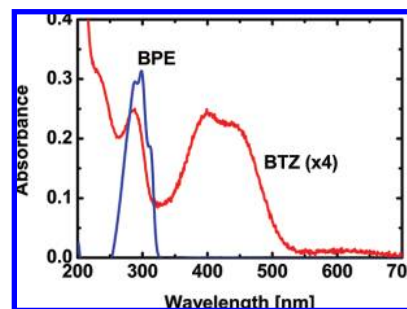
	$\tilde{\nu}_i$ (Raman) [ $\text{cm}^{-1}$ ]	bare $d\sigma/d\Omega$ [ $\text{cm}^2/\text{sr}$ ]	$\tilde{\nu}_i$ (SERS) [ $\text{cm}^{-1}$ ]	SMEF
BPE	1001	$2.6 \times 10^{-29}$	1010	$4.2 \times 10^{10}$
	1197	2.1	1202	4.8
	1343	1.4	1342	1.9
	1601	2.9	1608	3.4
	1641	5.5	1639	3.2
BTZ	1108	$1.0 \times 10^{-28}$	1134	$2 \times 10^{10}$
	1412	2.5	1410	1
	1617	0.87	1617	1
adenine	724	$2.9 \times 10^{-30}$	735	$7.1 \times 10^{10}$
$^{15}\text{N}$ -adenine	716	3.2	728	10.2

<sup>a</sup> Also shown are the corresponding typical maximum single-molecule SERS enhancement factors (SMEFs), representative of the largest SM-SERS events identified with the BiASERS method. Note that the results for BTZ are much more uncertain because most Raman/SERS peaks are relatively wide and part of a doublet. In the case of BPE, a single event exhibited SMEFs  $\sim 50\%$  larger than those shown here, but it was excluded from the analysis because of the lack of statistics on such rare events.

volume<sup>7</sup> of the  $\times 50$  objective was found by this method to be  $V_{\text{eff}} = 152 \mu\text{m}^3$ . To translate signals in “counts per second” into a differential cross section, a characterization of the throughput of the system is required with respect to a sample with a well-known Raman differential cross section. However, in contrast to measurement of the bare cross sections in liquid, for the experiments on solid substrates under an air objective, it is not possible to use the liquid 2-bromo-2-methylpropane as a reference. Accordingly, the SM signals, as identified by the bianalyte SERS procedure, were calibrated with respect to the signal of the  $2331 \text{ cm}^{-1}$  mode of nitrogen gas in air at room temperature and standard pressure (using long integration times). The  $2331 \text{ cm}^{-1}$  of  $\text{N}_2$  has a differential cross section of  $1.64 \times 10^{-31} \text{ cm}^2/\text{sr}$  at  $633 \text{ nm}$ .<sup>3,32</sup>

**Choice and Characterization of the Nonresonant SERS Probes.** As for resonant SM-SERS experiments, it is important that the SERS probe adsorbs efficiently on the metal surface of the substrate (silver in this study). This simplifies both the sample preparation and subsequent data analysis and interpretation. In this study, we initially consider two SERS probes that are known to attach efficiently to silver. The first one, purchased from Sigma-Aldrich, is 1,2-di-(4-pyridyl)-ethylene (BPE), which has been used repeatedly in SERS experiments in the past.<sup>33–35</sup> A benzotriazole dye, (3-methoxy-4-(5'-azobenzotriazolyl) phenylamine, dye no. 2 of ref 36 denoted BTZ here) was used as a BiASERS partner to BPE. It was synthesized as described earlier.<sup>36</sup>

Values of the experimentally obtained bare Raman differential cross sections for different modes of these two probes are summarized in Table 1. The UV–visible absorption spectra are also shown in Figure 2. Both molecules are nonresonant at  $633 \text{ nm}$  excitation, with BTZ absorbing close to the UV ( $\lambda = 427 \text{ nm}$ ) and BPE in the UV ( $\lambda = 300 \text{ nm}$ ). One could argue that BTZ still exhibits a small preresonant Raman effect at  $633 \text{ nm}$ , and this is indeed supported by the measurement of its differential Raman cross section of  $\sim 10^{-28} \text{ cm}^2/\text{sr}$  in water (see Table 1). However, we do not study specifically BTZ but merely use it as a convenient and well-understood BiASERS partner to BPE. In contrast, the absorp-

**Figure 2.** UV/vis spectra of BPE and BTZ molecules<sup>36</sup> taken at  $10 \mu\text{M}$  concentration. BPE was measured in ethanol because of its limited solubility in water. Both molecules are nonresonant at  $633 \text{ nm}$  laser excitation.

tion spectrum of BPE is a clear example of that of a nonresonant molecule. BPE was chosen here for its relatively large nonresonant Raman cross section  $\sim 10^{-29} \text{ cm}^2/\text{sr}$  in ethanol (see Table 1). This will allow us to first demonstrate nonresonant SM-SERS detection for the “easy” case of a good Raman scatterer before attempting to detect molecules representing the “worst” case of a small nonresonant molecule. In this case, adenine was selected for its importance in a biological context and because its SERS properties are well characterized.<sup>23,24,37</sup> The differential Raman cross sections of its main Raman modes are on the order of  $\sim 10^{-30} \text{ cm}^2/\text{sr}$  in water as seen in Table 1.

As a BiASERS partner to adenine, we use an isotopically substituted adenine, ( $^{15}\text{N}$ )<sub>2</sub>-1,3-adenine (henceforth referred to as  $^{15}\text{N}$ -adenine, purchased from Isotec, Sigma-Aldrich), for which the Raman/SERS spectrum is sufficiently different from that of (natural)  $^{14}\text{N}$ -adenine to distinguish them in a bianalyte SERS experiment (see later). The use of isotopically edited partners in combination with the bianalyte technique is arguably the ideal system for exploring SM detection as both probes have the same chemical characteristics in terms of surface adsorption and resonance properties.<sup>8,9</sup>

**SERS Substrate.** To minimize the presence of organic impurities, we prepared dried clusters of borohydride-reduced silver colloids on silicon as our SERS substrate. Following a modification of a previously reported synthesis,<sup>38</sup> KCl ( $7.9 \text{ mg}$ ,  $74.6 \text{ g mol}^{-1}$ ) was added to a solution of  $\text{AgNO}_3$  ( $18 \text{ mg}$ ,  $1.06 \text{ mM}$ ) in distilled water ( $80 \text{ mL}$ ) in a  $250 \text{ mL}$  round-bottomed flask equipped with a stir bar, with the resulting solution forming a cloudy blue precipitate of  $\text{AgCl}$ . The solution was cooled on ice, and an ice-cooled solution of  $\text{NaBH}_4$  ( $6 \text{ mg}$ ,  $37.8 \text{ g mol}^{-1}$ ) in distilled water ( $20 \text{ mL}$ ) was added in a single batch to the  $\text{AgCl}$  solution while the flask was shaken vigorously. Upon addition of the reductant, the solution became a cloudy yellow/gray color. The reaction was allowed to warm to room temperature and was kept stirring under a fume hood for 1 h to react excess  $\text{NaBH}_4$ . The resulting colloidal solution was stable for 2–4 weeks following preparation. For the SERS experiments, the colloids were concentrated after removal of the supernatant following centrifugation (by  $\sim 30$ -fold) and were then deposited on a Si substrate. In the preparation of the bare SERS substrate, a drop ( $50 \mu\text{L}$ ) of the concentrated colloids was placed on a Si wafer (drop area  $\sim 5 \times 5 \text{ mm}^2$ ), and the drop was evaporated with a blow gun. After evaporation, another drop was added and the process repeated three times (i.e., until the silicon surface was sufficiently covered). Next, the substrate was rinsed with distilled  $\text{H}_2\text{O}$  to try to remove as many contaminants from the borohydride system as possible. SERS was measured on these substrates close to the edge of the Si wafer, where the colloid surface coverage is larger as a result of the drying process.

To prepare samples of the analytes for SERS experiments, a drop ( $50 \mu\text{L}$ ) of the analyte solution at low concentrations ( $25 \text{ nM}$ ) was

(32) Schroetter, H. W.; Kloeckner, H. W. *Raman spectroscopy of gases and liquids*; Springer-Verlag: Berlin, 1979.

(33) Felidj, N.; Aubard, J.; Levi, G.; Krenn, J. R.; Hohenau, A.; Schider, G.; Leitner, A.; Aussenegg, F. R. *Appl. Phys. Lett.* **2003**, *82*, 3095.

(34) Aroca, R.; Corio, P.; Rubim, J. C. *Ann. Chim.* **1997**, *87*, 1.

(35) Freeman, R. G.; Bright, R. M.; Hommer, M. B.; Natan, M. J. *Raman Spectrosc.* **1999**, *30*, 733.

(36) Graham, D.; McLaughlin, C.; McAnally, G.; Jones, J. C.; White, P. C.; Smith, W. E. *Chem. Commun.* **1998**, 1187.

(37) Bernd, G.; McNaughton, D. *J. Phys. Chem. C* **2002**, *106*, 1461.

(38) Creighton, J. A.; Blatchford, C. G.; Creighton, M. G. *J. Chem. Soc., Faraday Trans.* **1979**, *2*, 790.

deposited onto the bare SERS substrate (drop area  $\approx 5 \times 5 \text{ mm}^2$ ) and allowed to stand for 30 min under ambient conditions. Finally, the drop was removed with a glass pipet, and the sample was rinsed in distilled  $\text{H}_2\text{O}$  before final drying. This method was effective in preparing low concentration samples of the nonresonant analytes without noticeable contamination. The final surface coverage/concentration of analyte cannot be determined with this method, but the single-molecule nature of the SERS signals can be assessed with the bianalyte technique, and the concentration adjusted accordingly if necessary.

**Linear Deconvolution Routine.** To select the valid events (from the large number of spectra measured), which may include erroneous spectra arising from photodegradation products or contaminants, the data were fitted by linear least-squares deconvolution, using as components the reference SERS spectra of BPE and BTZ, along with a linear background, i.e.,

$$I_{\text{BiASERS}}(\bar{\nu}_i) = \alpha I_{\text{BPE}}(\bar{\nu}_i) + \beta I_{\text{BTZ}}(\bar{\nu}_i) + \gamma \bar{\nu}_i + \delta \quad (1)$$

where  $I_{\text{BiASERS}}(\bar{\nu}_i)$  is the bianalyte SERS spectrum to be fitted and  $I_{\text{BPE}}(\bar{\nu}_i)$  and  $I_{\text{BTZ}}(\bar{\nu}_i)$  are those of the average SERS spectra obtained experimentally by individual measurement of the molecule under identical conditions.  $\alpha$ ,  $\beta$ ,  $\gamma$ , and  $\delta$  are the only fitting parameters and are uniquely (and easily) determined by the linear least-squares fitting routine. As the window selected for fitting was quite small ( $1580$  to  $1680 \text{ cm}^{-1}$ ), the inclusion of a linear background was sufficient to deal with any sufficiently broad fluctuating SERS background. This region was selected because the BPE and BTZ peaks in this region, although partially overlapping, were sufficiently distinct to allow adequate deconvolution while allowing for any slight shift in wavenumber (up to  $\sim 3 \text{ cm}^{-1}$ ), which occurs in typical SERS experiments. The validity of a fit (or “goodness-of-fit” value) was determined by a  $\chi^2$ -parameter, which was normalized to the spectral intensity of the event. Fits below a certain intensity (below noise level) and those with a “goodness-of-fit” below an appropriately chosen threshold were discarded along with any remaining nonphysical fits. The same analysis process was used for adenine experiments, but focusing on the relevant Raman shift window of  $700$  to  $780 \text{ cm}^{-1}$ .

This fitting process, in combination with suitable selection criteria, can effectively discard erroneous events arising from photodegradation and contaminants and, ultimately, recover the statistics of the two molecules of interest.

## Experimental Results

**Photodegradation Effects.** As pointed out in the introduction, a well-known phenomenon<sup>28</sup> is that there are limitations to the maximum amount of (laser) power we can deliver on the sample, particularly when focused on a dried substrate, before serious problems with photoinduced degradation on a subsecond time scale appear. The observation of photoproducts is particularly a problem for resonant or preresonant molecules if the photostability of the probe is poor (which is the case, for example, of dyes like malachite green<sup>39</sup>). But perhaps less intuitively, photodegradation in SERS experiments remains an issue for nonresonant molecules.<sup>13,29</sup> Reference 29 shows explicitly how the photochemistry of degradation of aromatic nonresonant species evolves in time, resulting eventually, after some transient intermediate states, into a final photoproduct that is similar to amorphous carbon in its spectral characteristics (but with some of the details being determined by the exact precursor<sup>29</sup>). We observe exactly the same in our case at high power densities ( $\sim 5 \text{ mW}$  focused onto a  $1.4 \mu\text{m}$  waist beam by the  $\times 50$  air objective). At this power level we see transient photoproducts on a subsecond time scale with randomly occurring peaks in the range characteristic of typical organic moieties with  $\text{sp}^2$ – $\text{sp}^3$  hybridizations of carbon, with a spectrum tending toward “amorphous-carbon-like” for long expositions to the laser on the

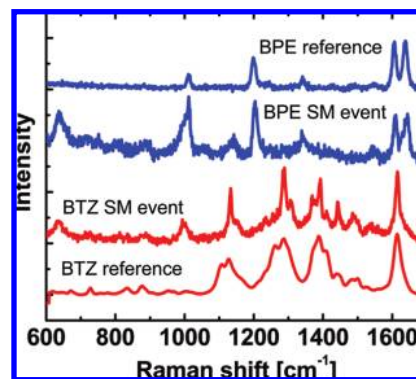


**Figure 3.** Example of individual SM-SERS events of BPE and BTZ along with average SERS spectra obtained by measurement of each analyte separately. From these SM-SERS events, and a careful characterization of the optical setup<sup>7</sup> and bare differential cross sections, the single-molecule enhancement factors are then obtained. The spectral features at  $\sim 633$ ,  $1100$ , and  $1550 \text{ cm}^{-1}$  in the SM-SERS events are also observed in spectra of the bare SERS substrate and do not belong to BTZ or BPE.

same spot. We find that (in our experimental conditions) a reasonable power to use was ( $\sim 0.5 \text{ mW}$  focused onto a  $1.4 \mu\text{m}$  diameter beam by the  $\times 50$  air objective) producing signals which remain stable for  $\sim 1 \text{ s}$  without too many events with obvious signatures of photodegradation. These parameters then fix the minimum differential cross section that can be observed in this case, as discussed extensively in ref 16. All SERS maps were thus taken under these laser conditions for moderate integration times of  $1 \text{ s}$ .

**Evidence of Single-Molecule Detection.** Having identified suitable conditions for the BTZ/BPE system, bianalyte SERS maps were taken of substrates prepared in the manner described before. A credible demonstration of bianalyte SERS should be able to isolate single analyte events of the two complementary probes. From 4900 spectra, it was possible to identify 326 events that passed the noise and “goodness of fit” thresholds. Figure 3 shows examples of the SM spectra of BPE and BTZ, along with the (reference) average SERS spectra of each molecule obtained individually. For the BTZ SM-event, it can be seen that the spectral resolution of the vibrational modes is somewhat narrower for the SM event than for the reference spectra. BTZ Raman peaks are almost all doublets, and this narrowing may therefore be attributed to different relative intensities within a doublet (as a result of surface selection rules, for example). Studies by other authors<sup>8</sup> have also suggested that such narrowing is a characteristic of single-molecule spectra, even though in our opinion the exact origin of the line widths has to be analyzed in general with uttermost care (because it can include instrumental components, like the exact position of the image on the entrance slit of the spectrometer for different events). We make no attempt here to interpret the linewidths but rather concentrate on the standard BiASERS analysis<sup>1</sup> and therefore focus on the integrated intensity of the peaks. Figure 4 shows the corresponding intensity histogram of these events, where the abscissa shows the relative contributions of each reference spectra to the bianalyte SERS spectra. From the histogram, it can be seen that there are 79 SM events of BPE (right end of the histogram) and 66 of BTZ (left end of the histogram) in the map.

It is worth noting that these numbers do not necessarily have the normal statistical meaning as in the standard bianalyte SERS of resonant or preresonant probes, for there are many signals (of both types) that are not actually counted because they are contaminated with spurious photoproduct signals, i.e. peaks that belong to unidentified carbonaceous species.<sup>29</sup> On the contrary, these numbers represent the random chances of finding a “clean” signal in a background of spurious (and comparable in size) peaks. Notably, the chances of finding each analyte as a single molecule are equivalent, and situations in between are randomly distributed.

(39) Domke, K. F.; Pettinger, B. *Phys. Rev. B* **2007**, *75*, 236401.

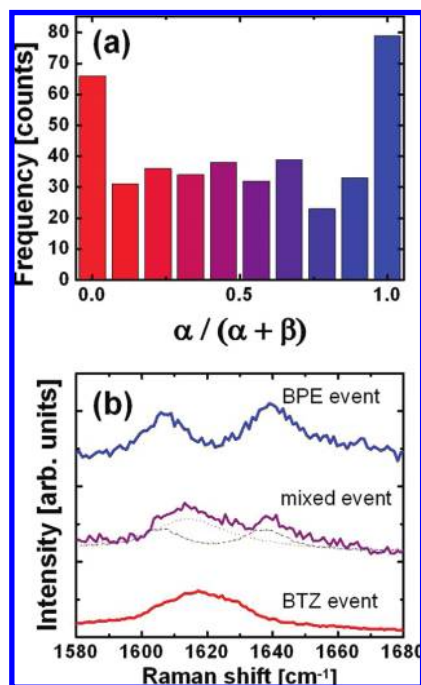


**Figure 4.** (a) Histogram showing relative proportions of the two reference spectra (BPE ( $\alpha$ ) and BTZ ( $\beta$ )) in making up the experimental events that have been identified as valid spectra. The abscissa ( $\alpha/(\alpha + \beta)$ ) represents the fraction contributed to the spectrum by BPE (i.e.,  $\alpha/(\alpha + \beta) = 0$  means “pure BTZ”,  $\alpha/(\alpha + \beta) = 1$  means “pure BPE”). The larger relative number of single-molecule events of either molecule indicates we are entering the single-molecule regime.<sup>6</sup> In (b) we show three representative cases of a pure BTZ or BPE spectrum, with a mixed spectrum containing contributions from both dyes. The linear deconvolution is done in the 1580–1680  $\text{cm}^{-1}$  range, which contains distinguishable Raman fingerprints for both dyes.

This indicates that we are effectively entering into the single-molecule regime as defined by the bianalyte technique.<sup>6</sup>

**Single-Molecule SERS Enhancement Factors for BPE.** Having identified single-molecule signals, we can now obtain SM enhancement factors (SMEFs) after characterization of the objective and measurement of the 2331  $\text{cm}^{-1}$  mode of  $\text{N}_2$ , performed under the same conditions as those in the experiment (see section for details). There is obviously no single EF for all SM events but rather a distribution of EFs for single molecules in different conditions. From the range of SM events observed, we focus on the maximum EFs, i.e. those estimated from the first few largest SM-SERS events (example in Figure 3). The results are summarized in Table 1. We obtain maximum SMEFs in the range of  $1 \times 10^{10}$ – $5 \times 10^{10}$  for both BTZ and BPE. Notably, however, there were also SM events detected with smaller EFs, down to  $\sim 5 \times 10^9$  for the nonresonant molecule BPE. Being able to see these events at EFs below the maximum achievable EFs for our system naturally suggests the possibility of observing nonresonant molecules with lower intrinsic cross sections (by a factor of  $\sim 5$ – $10$ ).

It is important to realize that these values come from (i) independent characterization of the bare probes, which implies a full calibration with respect to a reference in liquid (2B2MP), and (ii) comparison of the SM-SERS cross section with respect to another reference (nitrogen gas). The fact that all these determinations can be put together to produce a number which is perfectly in agreement with the expectations of maximum enhancement factors at hot spots is quite remarkable in itself, and it shows a pleasing consistency of the underlying physics of the effect, which has been for many years elusive due to the uncertainty in the number of molecules being measured. This is the specific aspect that the bianalyte technique solves, thus opening the possibility for quantitative comparisons that would not be feasible otherwise.

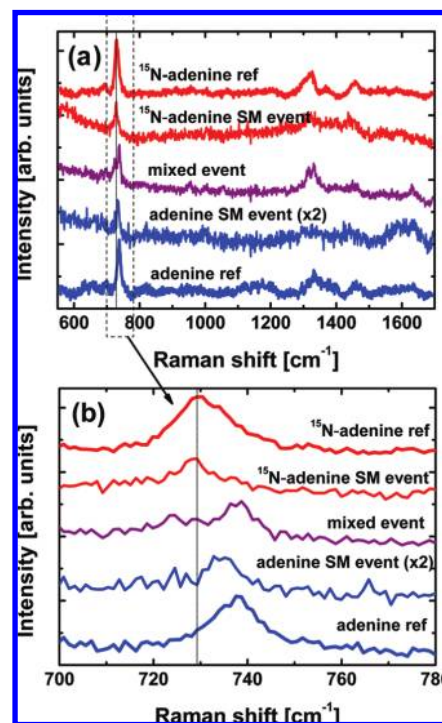


**Figure 5.** (a) SM events of adenine and  $^{15}\text{N}$ -adenine along with a mixed event identified from a BiASERS map. The reference average SERS spectra of each molecule are also shown. The adenine/ $^{15}\text{N}$ -adenine bianalyte SERS experiment was performed using the same substrate preparation and experimental conditions as the BTZ/BPE results. (b) Expansion of the 700–780  $\text{cm}^{-1}$  range for the spectra in (a). This was also the range used in performing linear deconvolution of the bianalyte spectra to analyze the SM events.

It is also worth noting the small discrepancy in maximum SMEFs measured for different Raman modes of the same molecule or between those of BTZ and BPE. One obvious interpretation for the latter is the presence of a small additional chemical enhancement factor (on the order of  $\sim 2$ – $4$ ) for BPE. However, other mechanisms could also cause this small discrepancy, including the following: (i) BTZ could be more susceptible to photodegradation than BPE, and although not observable as distinctive amorphous carbon features in the SERS spectra, it is possible that the SMEFs of BTZ are limited in the highest EF cases by photodegradation within our integration time. (ii) Surface selection rules<sup>3,40,41</sup> could also result in small discrepancies of this order between Raman modes of a molecule or between two different analytes. We cannot conclude from our results here which mechanism (or combination of them) is at play.

**Single-Molecule SERS of Adenine.** Having determined that our system can indeed provide hot spots with enhancement factors toward the upper end of those available, we next measured adenine along with its isotopically edited bianalyte SERS partner,  $^{15}\text{N}$ -adenine, using the same preparation methodology and experimental conditions. Again, a map of the substrate was taken with a large number of spectra (5535) and single-molecule events were identified by linear deconvolution of adenine and  $^{15}\text{N}$ -adenine reference spectra measured individually, along with a linear background. The reduction in intrinsic cross section was immediately noticeable, with a much greater proportion of events dominated by spurious signals, from either contaminants or photodegradation processes. For this reason, it was not possible to find as many single-molecule events as with the other probes.

(40) Moskovits, M. *J. Chem. Phys.* **1982**, *77*, 4408.

(41) Le Ru, E. C.; Meyer, M.; Blackie, E.; Etchegoin, P. G. *J. Raman Spectrosc.* **2008**, *39*, 1127.

Nonetheless, several examples of SM events of each molecule could be isolated (at the expense of a much larger sampling) as shown in Figure 5. In this case, it was not possible to obtain SMEFs for most of the modes because individual peaks were difficult to resolve in the SM-SERS spectra. It was possible, however, to get good fits for the peak at  $\sim 735\text{ cm}^{-1}$  for adenine ( $\sim 728\text{ cm}^{-1}$  for  $^{15}\text{N}$ -adenine) and to obtain representative maximum SMEFs for these modes (see Table 1). These maximum SMEFs, at  $7 \times 10^{10}$  and  $1 \times 10^{11}$ , are consistent with the BPE results and represent the uppermost end of EFs available in our system. In the case of adenine, these are also the minimum SMEF for which SM-SERS events could be detected.

## Discussion and Conclusions

Maximum enhancement factors in the range  $\sim 10^{10}$ – $10^{11}$  are perfectly within reach of classical electromagnetic theory of gap plasmon resonances.<sup>3,11,16,18–21</sup> Like many situations in SERS, it is conceivable that this number has a small contribution from a “chemical enhancement”.<sup>42</sup> The observed frequency shifts are, in fact, sometimes an indication that a small chemical component of the enhancement might be present through the interaction of the molecule with the substrate. But it is not the main topic here to separate the relative contributions of the “electromagnetic” and “chemical” enhancements (which we cannot separate unambiguously in any case) but rather to point out that enhancement factors of  $\sim 10^{10}$ – $10^{11}$  can actually be used to see single molecules with some of the smallest differential cross sections. Accordingly, these results demonstrate that it is possible to detect nonresonant probes with intrinsic Raman cross sections down to  $\sim 10^{-30}\text{ cm}^2/\text{sr}$ . In that sense (as pointed out in the introduction) we see our study here as a fundamental

*proof of principle* of the minimum yardstick detection level of the technique at the single-molecule level.

The possibility of utilizing SM-SERS with other nonresonant molecules of interest could only be decided on a case-by-case basis, depending on the stability of the molecules under given experimental conditions and the likelihood of spurious “carbonaceous” species of comparable weak cross sections (plus additional possible problems with photostability). However, we have shown here that, with the right preparation conditions and suitable selection of experimental conditions, it is indeed possible to see SM events of nonresonant molecules. The conditions involve an inevitable compromise between laser power, integration time, and sample preparation. The results presented here suggest that, under the right conditions, differential cross sections on the order of  $\sim 10^{-30}\text{ cm}^2/\text{sr}$  are indeed measurable, and this would be approaching the lowest detection limit of the technique at the single-molecule level. As many of the molecules of widespread interest fall into this category, this offers interesting possibilities. If all experimental problems are resolved, we are forced to conclude that (in principle) *any* molecule that can be made to adsorb on the substrate can be observed at the single-molecule level with SERS. This is a statement that has been made several times in the literature in different contexts but never with proper justification through a specific quantitative example. We believe the results presented here provide a conclusive demonstration of SM-SERS for nonresonant probes and sets the claim on the lowest detection limit of single molecules in SERS on firm footing.

**Acknowledgment.** P.G.E. and E.C.L.R. acknowledge partial support for this research by the Royal Society of New Zealand (RSNZ), through a Marsden Grant.

JA905319W

(42) Tian, Z. Q. *Faraday Discuss.* **2006**, *132*, 309.